

Use of single station observations:
data quality control and the noise field in Europe.

Helle Pedersen, Yang Lu, Laurent Stehly, Anne Paul, Nicolas Leroy, Dimitri Zigone,
Martin Vallée, Adam Ringler, David Wilson & the AlpArray Working Group

Use of single station observations:

Part I: Quality control with component ratios : 20 years of GEOSCOPE data

Helle Pedersen, Nicolas Leroy, Dimitri Zigone, Martin Vallée,
Adam Ringler & David Wilson

Why we do this...

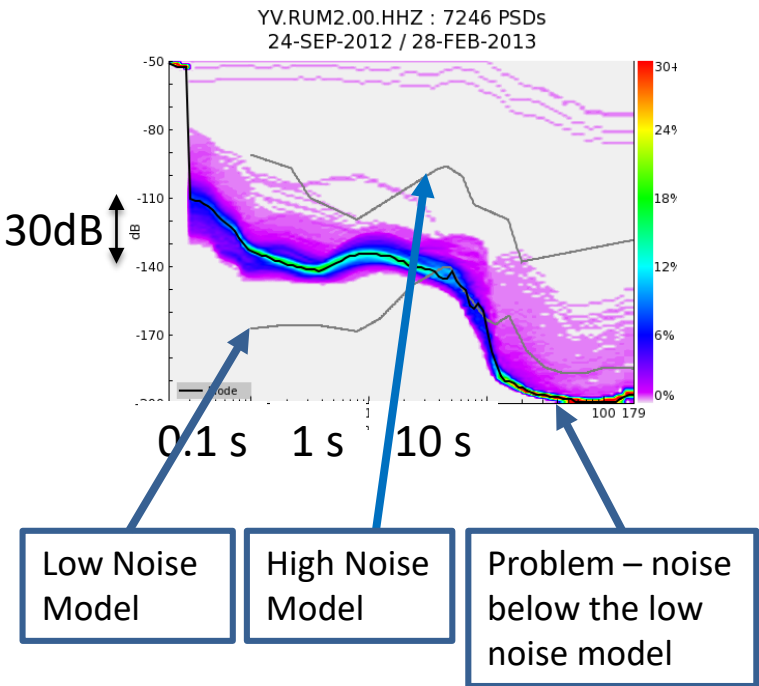
- Scientific users need to be able to evaluate data quality in spite of vast of data volumes – **automatic tools** for data rejection are needed
- Network operators need to be able to identify and correct instrument and metadata problems – **simple and/or automatic tools** are very valuable

But... it is not an easy task as there are many different instrument problems to handle

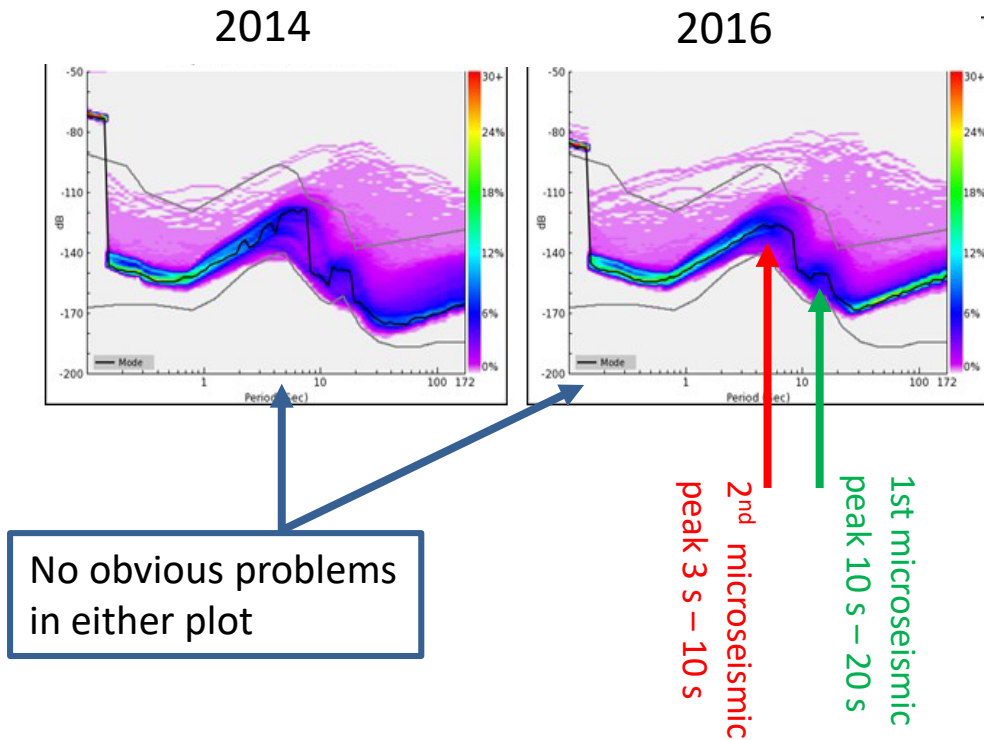
Here we focus on inconsistencies between different components of motion

Standard visualization: Power spectral density

Example RHUM-RUM temporary experiment, stat RUM2



Example of permanent permanent station Echéry (ECH), where reinstallation took place in 2015.



Method: use H/V ratios for fine characterization of incoherency between components

Method:

- Download daily files
- Dmean, detrend, prefilter, decimate, deconvolve with instrument respons
- Rotate to ZNE if necessary
- Cut into 5 min windows
- Calculate the average Energy of each component in each window, for 8 different frequency bands
- Calculate the ratio of Energy between the three components (E/Z,N/Z,E/N)
- Calculate the three **median** energy ratios over the 288 time windows of the day (reduce influence from earthquakes)

Data used:

- Network G: Institut de Physique du Globe de Paris and Ecole et Observatoire des Sciences de la Terre de Strasbourg (EOST), 1982.
- Network IU: Albuquerque Seismological Laboratory (ASL)/USGS, 1988.

How to cite seismic data

Citing is based on network code.

If the network has a DOI: Refer to the data as you would to a normal scientific manuscript, and include the reference in the normal list of references.

Network, citation and DOI information can be found at <http://www.fdsn.org/networks/>

If many networks are used: most journals accept a 'Data Section'

Example:

'We used data from GEOSCOPE (Institut De Physique Du Globe De Paris (IPGP) and Ecole Et Observatoire Des Sciences De La Terre De Strasbourg (EOST), 1982) and GEOFON (Geofon Data Centre, 1993).'

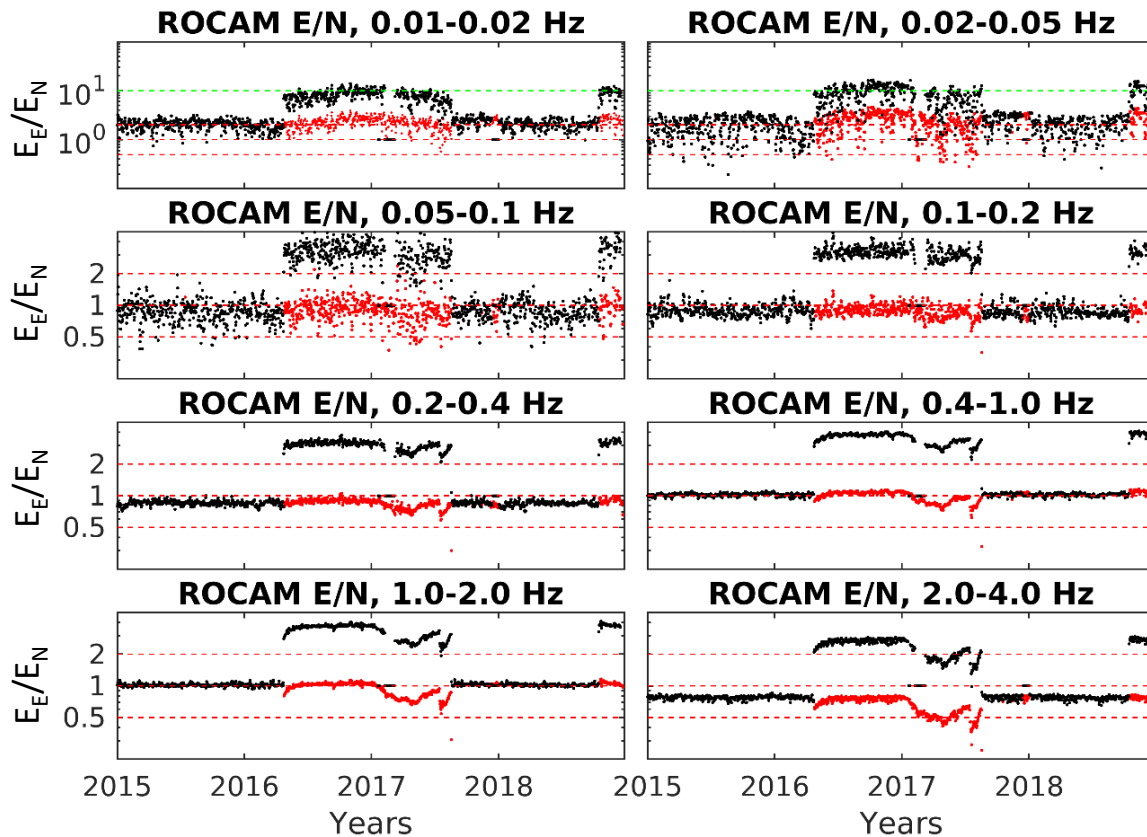
References:

GEOFON Data Centre, 1993. GEOFON Seismic Network. Deutsches GeoForschungsZentrum GFZ.

<https://doi.org/10.14470/tr560404>

Institut De Physique Du Globe De Paris (IPGP), & Ecole Et Observatoire Des Sciences De La Terre De Strasbourg (EOST), 1982. GEOSCOPE, French Global Network of broad band seismic stations. Institut de Physique du Globe de Paris (IPGP). <https://doi.org/10.18715/geoscope.g>

Example results: amplitude problem at station ROCAM

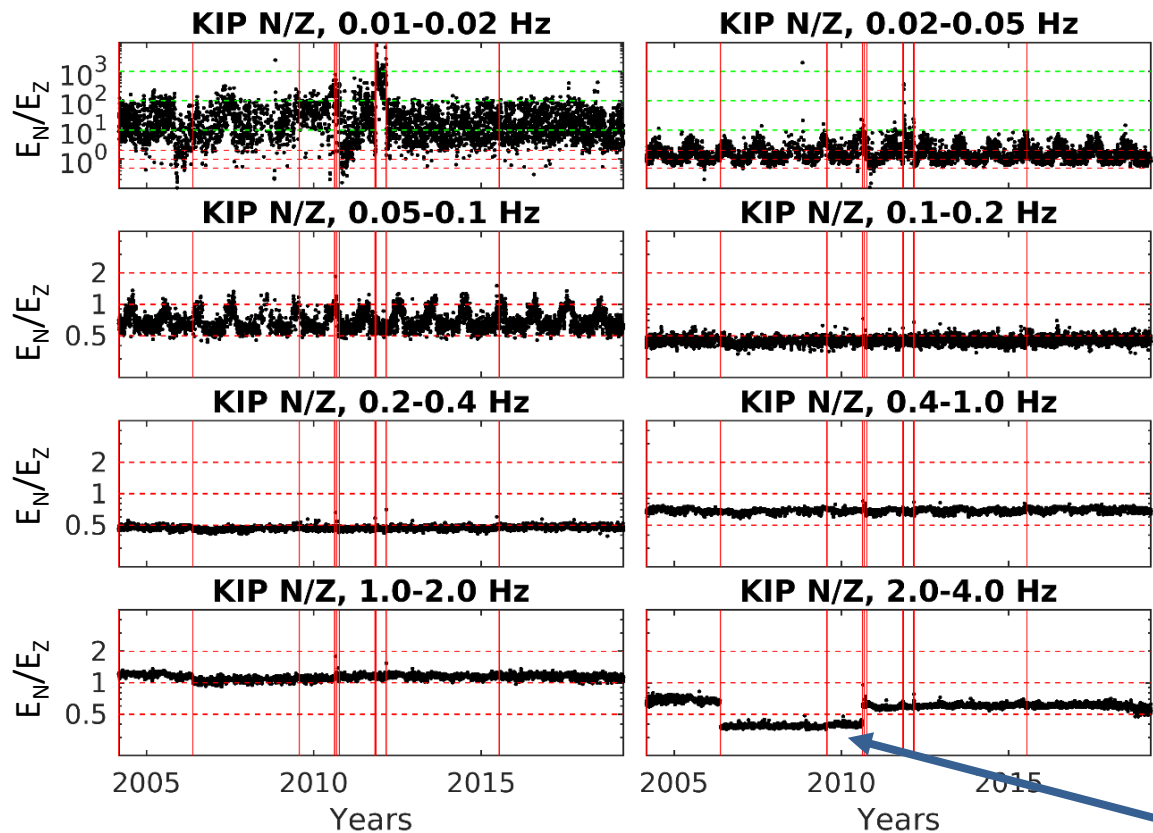


Gain problem between Q1 2016 and mid-2017

Corrected using this method

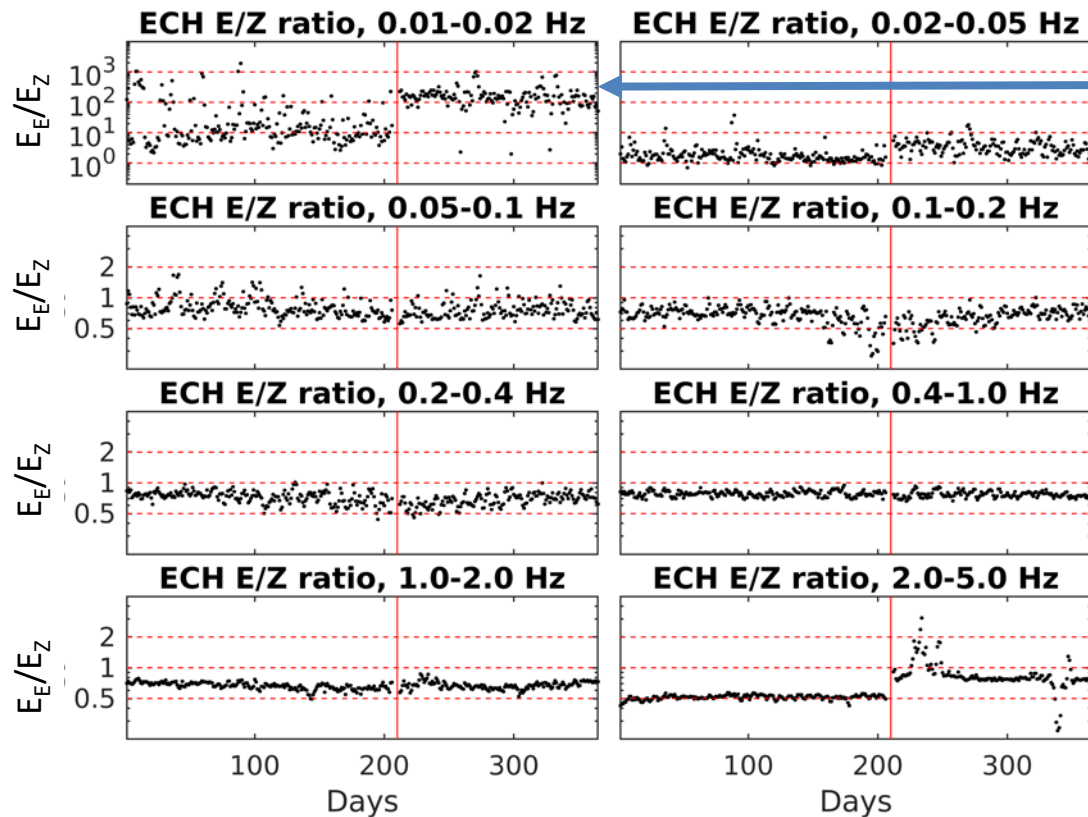
Black points: uncorrected
Red points: corrected

Example results: instrument response problem at station KIP (code share IU USGS)



Temporary problem with instrument response - probably erroneous at frequencies > 1Hz

Example results: 2 independent problems at station ECH



Low frequencies:
Abrupt change
Likely cause:
deterioration of E
component at
reinstallation

High frequencies:
Abrupt change
Likely cause: error in
instrument response for
frequencies > 1Hz

Conclusions Part I

Don't expect data to be perfect: visually check as much data as relevant or possible, and automatically apply relevant quality criteria - across all frequency bands that you use

Cite data correctly using DOIs when available

Use of single station observations:

Part II: Microseismic noise across Europe

Helle Pedersen, Yang Lu, Laurent Stehly, Anne Paul & the AlpArray Working Group

Why we do this...

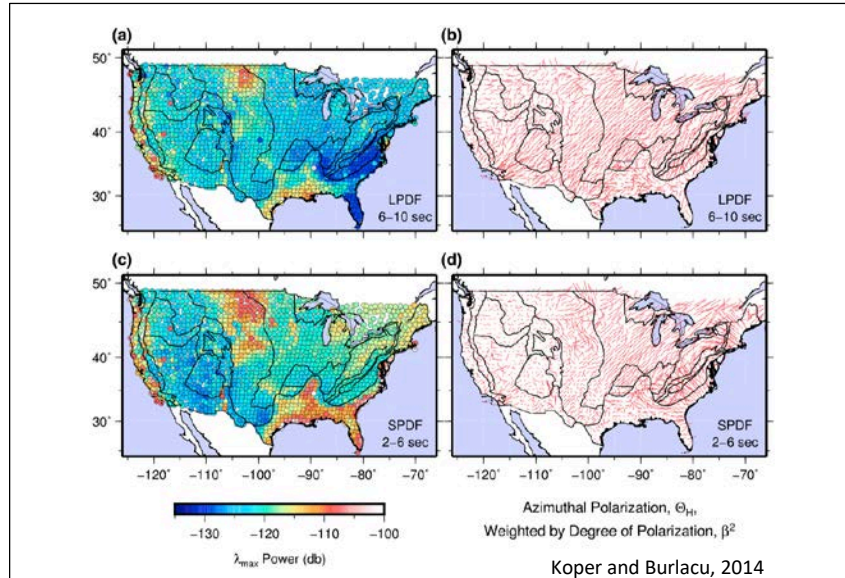
- Extracting the Green's function from seismic noise is based on an assumption of diffuse noise or well distributed noise sources – but this is not true
- Additional difficulty: the noise field varies in space and time
- The more we know about the noise field, the more intelligently we can use it for imaging in 2D, 3D and 4D

Here we focus on **spatial and temporal variations of the noise in Europe** – extracting some characteristics that we believe are informative

Using single stations: hugely underdetermined problem

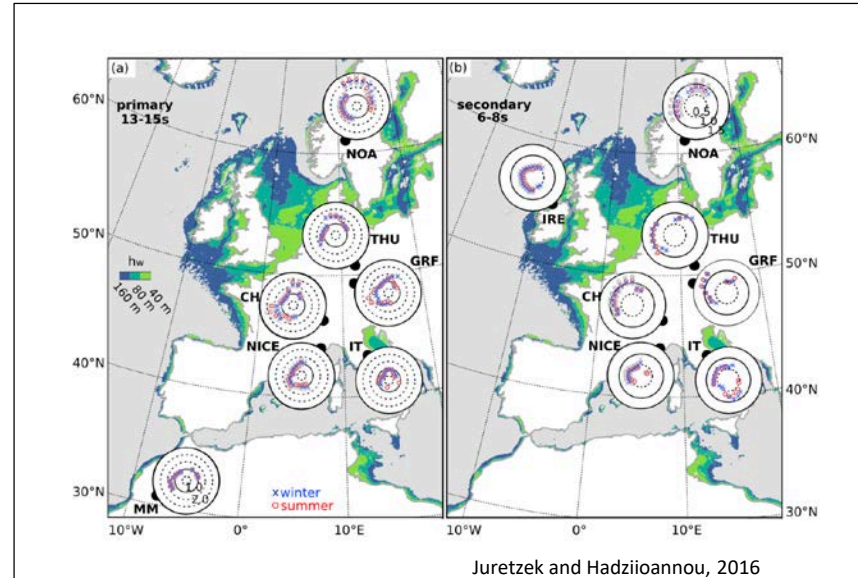
Goal: characterize the microseismic noise across Europe, and its seasonal variations

Single station observations in USA



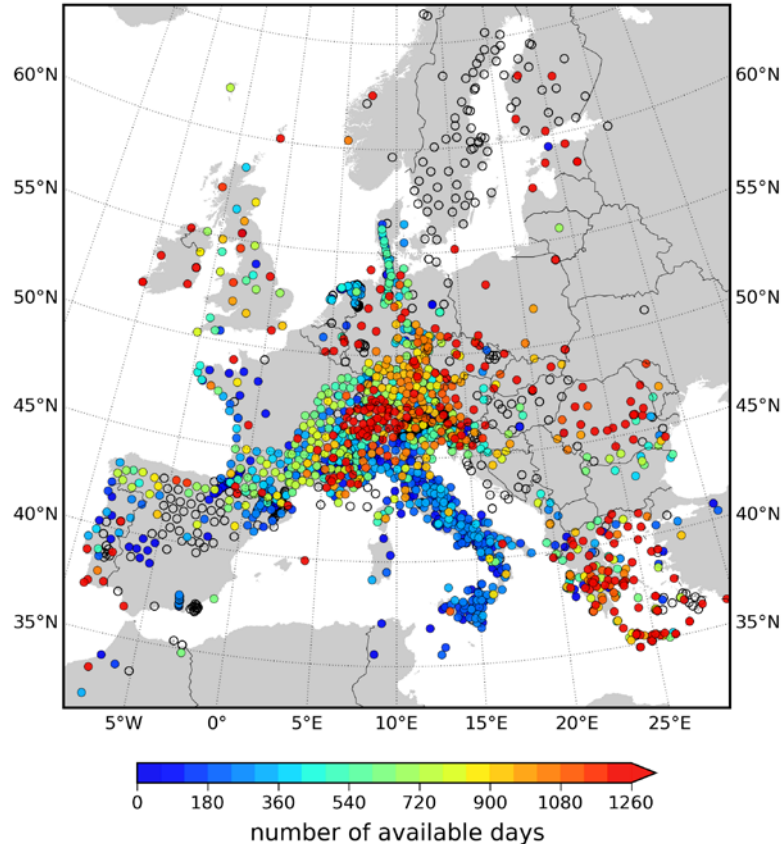
- 1) Noise energy influenced by both structure and noise sources; Coherent azimuth patterns
- 2) Increased spatial complexity for higher frequencies

Array observations in Europe



- 1) Love waves dominate on average, especially in the primary microseismic peak
- 2) NW dominating source areas with spatial variability

Data : long time series and high station density in the wider Alpine area



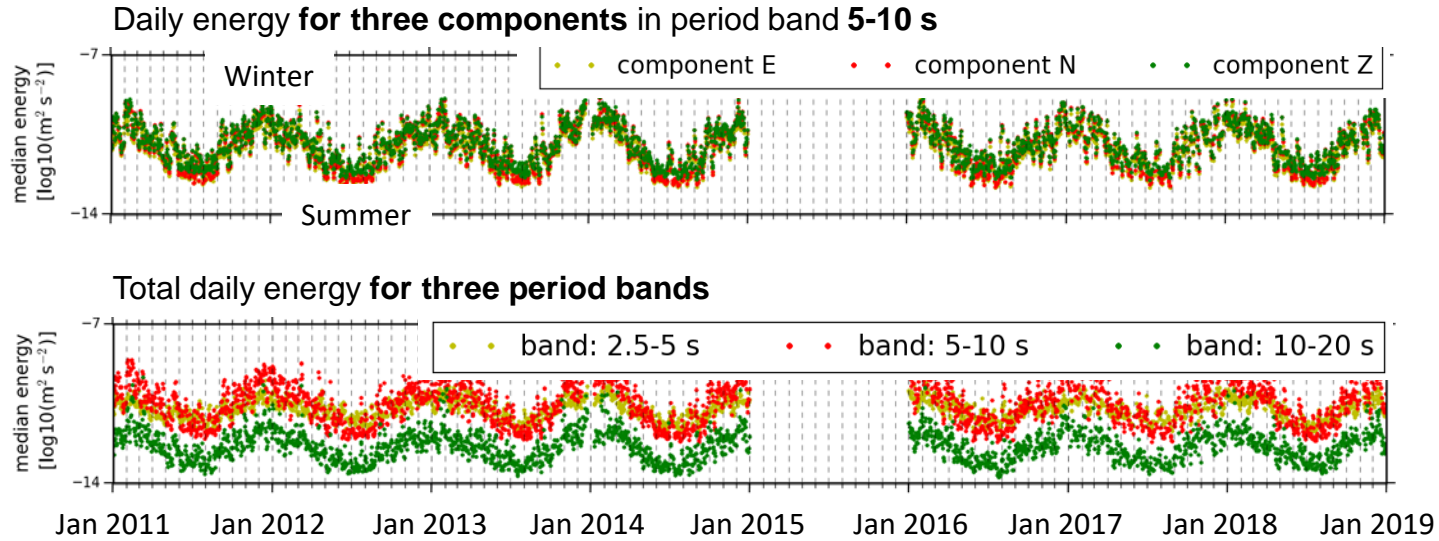
2476 seismic stations (permanent and temporary) operated in the 7 years of 2011, 2012, 2013, 2014, 2016, 2017, 2018;

1648 seismic stations have available data;

222 seismic stations have ≥ 3.5 years (1260 days) of data.

Standard preprocessing and downsampling to 1 Hz

Energy: example from the Alps

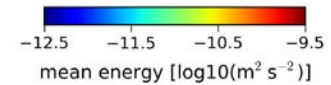
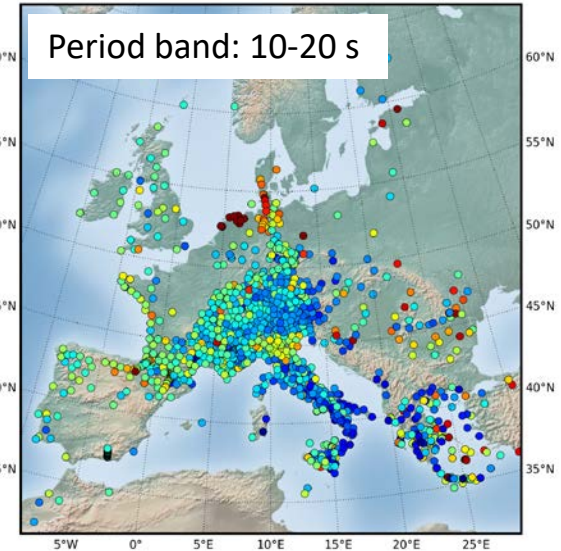
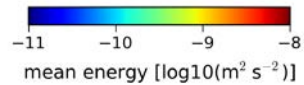
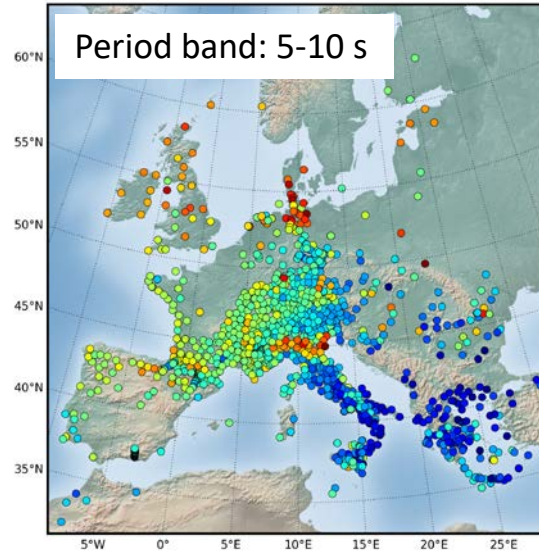


Daily measurements are calculated in each period band by the **median** value of measurements on up to 144 non overlapping windows (10 min windows)

In each 10 min window, energy for i th component is calculated as: $E_i = \frac{1}{N} \sum_{j=1}^N (u_{i,j})^2$ u : velocity; N : number of samples in the window .

Total energy for each period band is calculated as the sum of energy for three components: $E = \sum_{i=1}^3 E_i$

Spatial distribution of energy (mean over daily measurements 2011-2018)

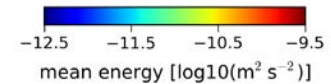
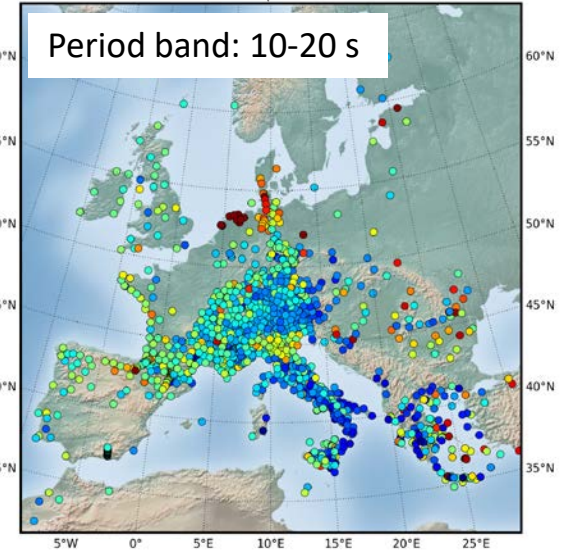
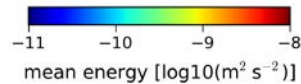
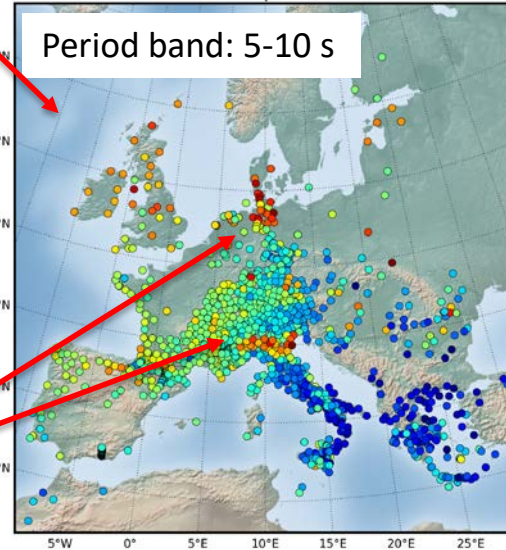


Spatial distribution of energy (mean over daily measurements 2011-2018)

Energy gradient
from source
direction

Variations are dominated by distance to source; some effect of structure

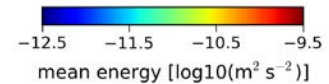
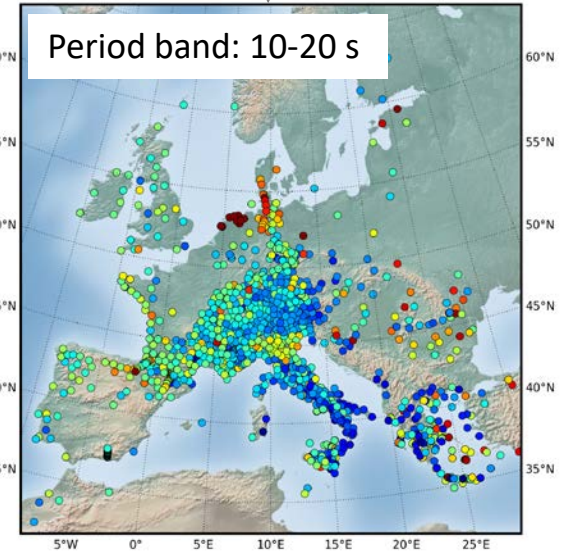
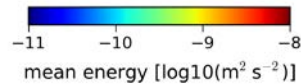
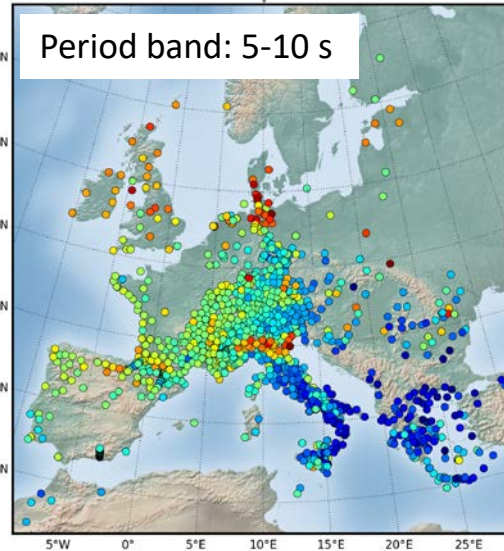
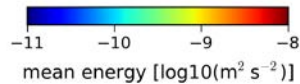
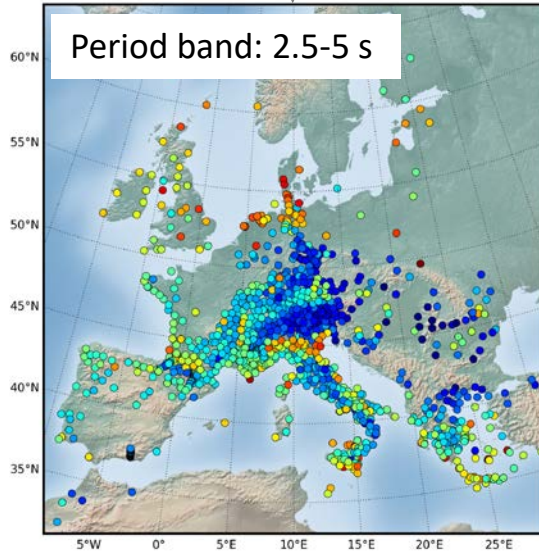
Effect of deep basins



Spatial distribution of energy (mean over daily measurements 2011-2018)

Variations are strongly influenced by structure

Variations are dominated by distance to source; some effect of structure



Temporal variation of energy for 3 networks (2018) at 5 s -10 s period

Peaks are strongly related to ocean activity in the North Atlantic

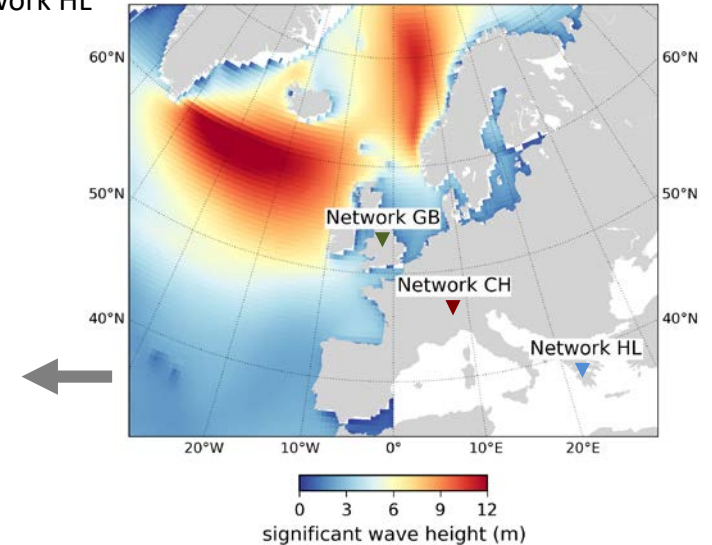
Network GB

Network CH

Network HL

Date: 2018-01-15 (winter)

Mean wave height in the North Atlantic



GB: Great Britain Seismograph Network.

CH: Swiss Seismological Service (SED) at ETH Zurich (1983).

HL: National Observatory of Athens Seismic Network (1997).

Wave height data are from *NOAA WAVEWATCH III*.

Temporal variation of energy for 3 networks (2018)

Peaks are strongly related to ocean activity in the North Atlantic

Network GB

Network CH

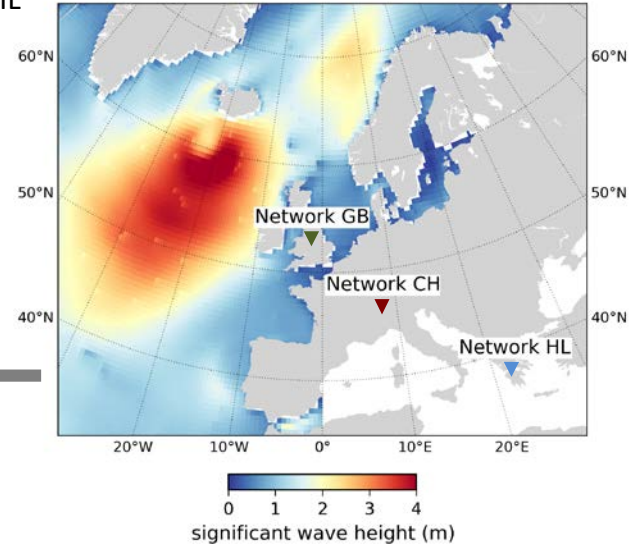
Network HL



Mean wave height in the North Atlantic



Date: 2018-07-15 (summer)



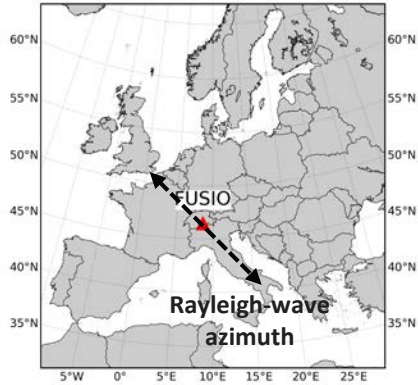
GB: Great Britain Seismograph Network.

CH: Swiss Seismological Service (SED) at ETH Zurich (1983).

HL: . National Observatory of Athens, Institute of Geodynamics, Athens (1997)

Wave height data are from *NOAA WAVEWATCH III*.

Rayleigh and Love waves: example from the Alps



Rayleigh waves incident direction:
Identifying the direction for which
there is a 90° phase shift with the
vertical component

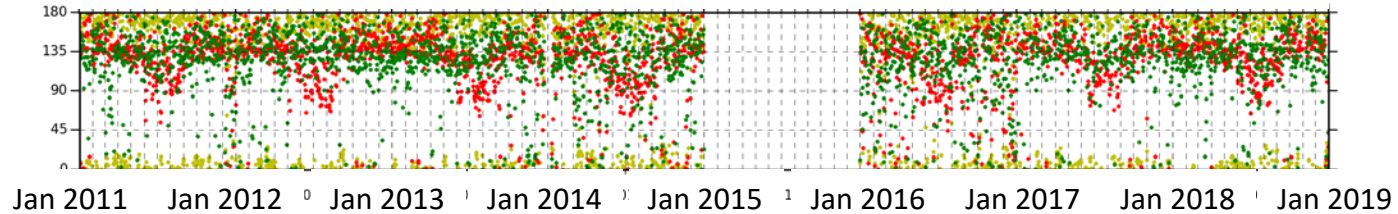
Rayleigh-wave azimuth is defined as:

$$\underset{\theta}{\operatorname{argmin}}[|\varphi_{VR}(\theta) - 90^\circ|]$$

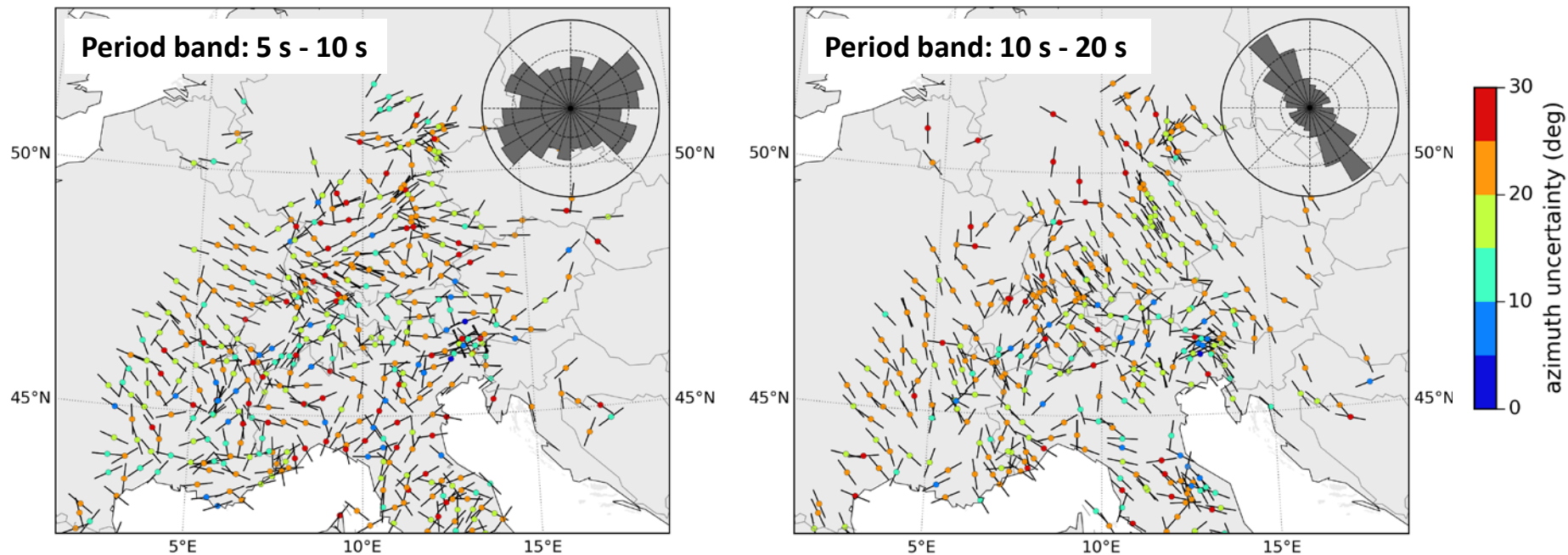
where φ_{VR} is the vertical-radial
phase difference in degree.

• • band: 2.5-5 s • • band: 5-10 s • • band: 10-20 s

Daily Rayleigh-wave azimuth

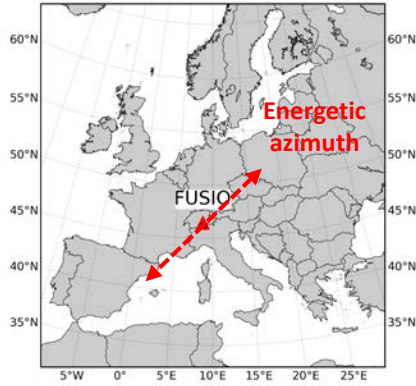


Azimuth of Rayleigh waves (mean over daily measurements 2011-2018)



- 1) Clear source direction (NW) in first microseismic peak (10 s – 20 s)
- 2) Complex noise wavefield in secondary microseismic band (5 s - 10 s)
- 3) Azimuth uncertainties (one standard deviation) are mostly between 15°-20° → strong temporal variation.

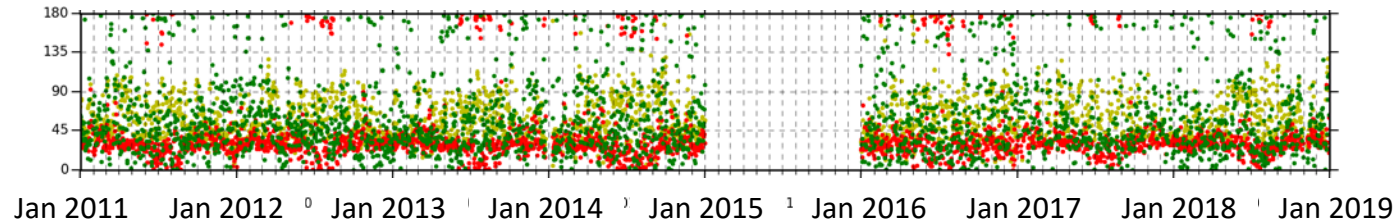
Rayleigh and Love waves: example from the Alps



Energetic azimuth is calculated based on the eigenvalue decomposition of the covariance matrix of three components. Eigenvalues $(\lambda_1, \lambda_2, \lambda_3)$ and eigenvectors (v_1, v_2, v_3) are solutions of $(\text{cov}[u_E, u_N, u_Z] - \lambda^2 I)v = 0$ and sorted so $\lambda_1 > \lambda_2 > \lambda_3$. The energetic azimuth (most important horizontal orientation of particle motion) is given by $\tan^{-1}(v_{21}/v_{11})$ (Flinn, 1965).

• • band: 2.5-5 s • • band: 5-10 s • • band: 10-20 s

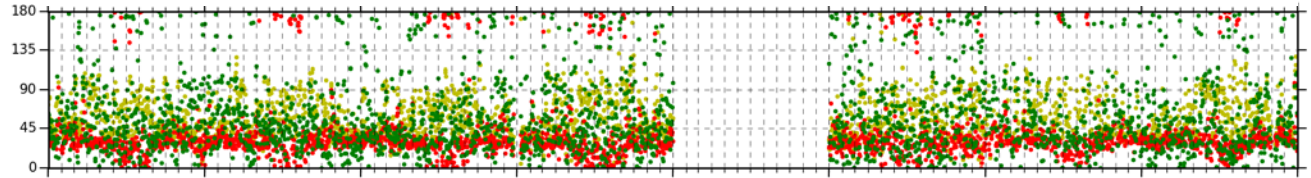
Daily dominant energy azimuth



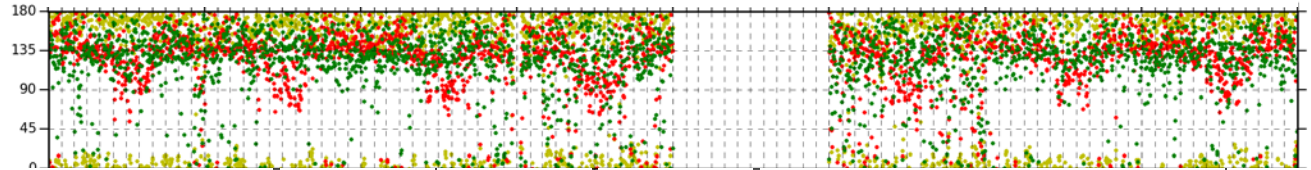
Rayleigh and Love waves: example from the Alps

• • band: 2.5-5 s • • band: 5-10 s • • band: 10-20 s

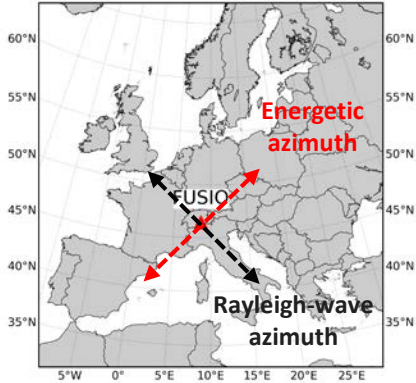
Daily energetic azimuth



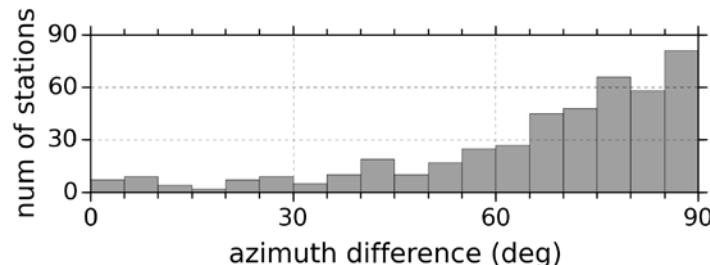
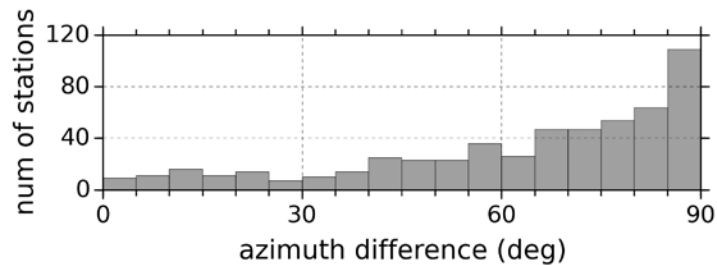
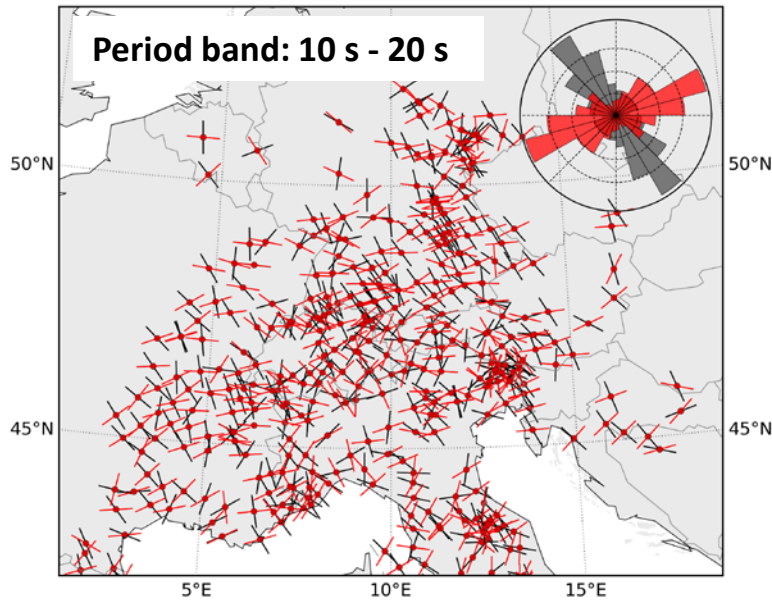
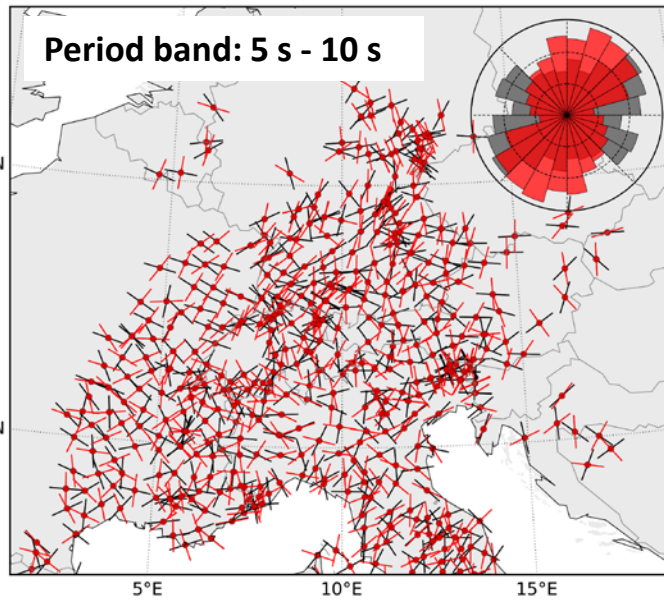
Daily Rayleigh-wave azimuth



Jan 2011 Jan 2012 Jan 2013 Jan 2014 Jan 2015 Jan 2016 Jan 2017 Jan 2018 Jan 2019



Dominant energy azimuth (mean over daily measurements 2011-2018)



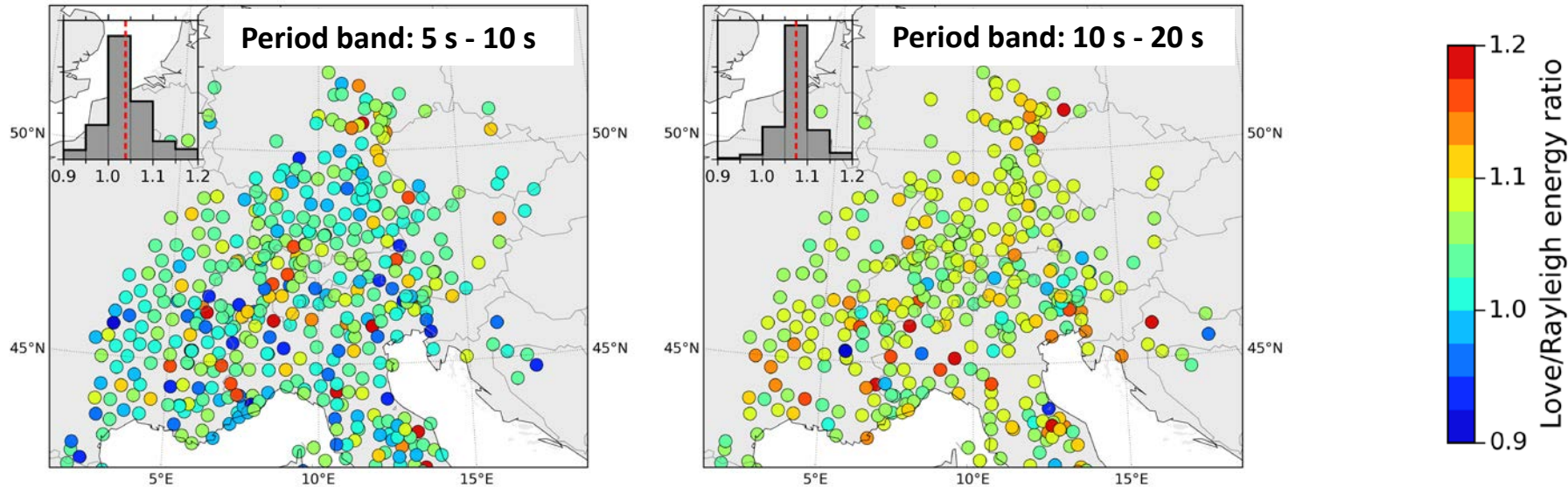
Dominant energy azimuths are ~perpendicular (60° - 90°) to the Rayleigh wave azimuths.



Love waves dominate in both period bands

We can calculate the approximate ratio $\text{Hor}_L/\text{Hor}_R$

Love / Rayleigh wave ratio of horizontal components based on single station observations



Love/Rayleigh wave ratio is defined as : $ratio = E_{\theta} / E_{\theta+90}$, where θ is Rayleigh-wave azimuth, and $\theta+90^{\circ}$ is an estimate of Love-wave azimuth.

Love waves dominate on average with mean Love/Rayleigh wave ratio **1.04** in the secondary microseismic period band (5 s -10 s) and **1.07** in primary microseismic period band (10 s - 20 s).

No influence of distance to seismic noise source, no influence of structure

Body waves: indications of significant relative amplitudes in summer through H/V



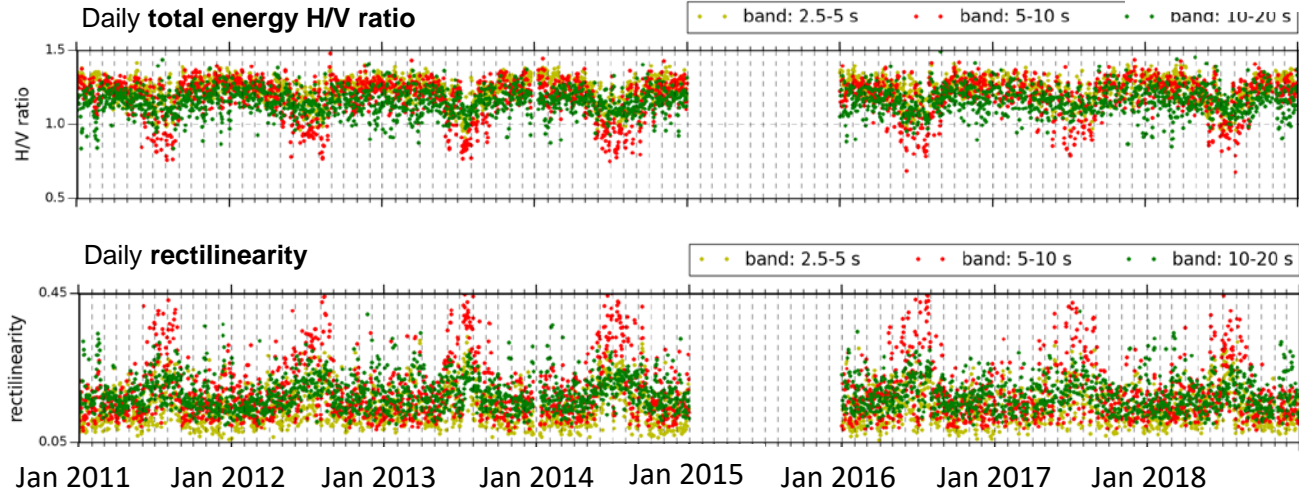
Total energy H/V ratio is given by:

$$\text{ratio} = (E_E + E_N) / E_Z$$

Rectilinearity is given by:

$$\text{rectilinearity} = 1 - \sqrt{\lambda_2 / \lambda_1}$$

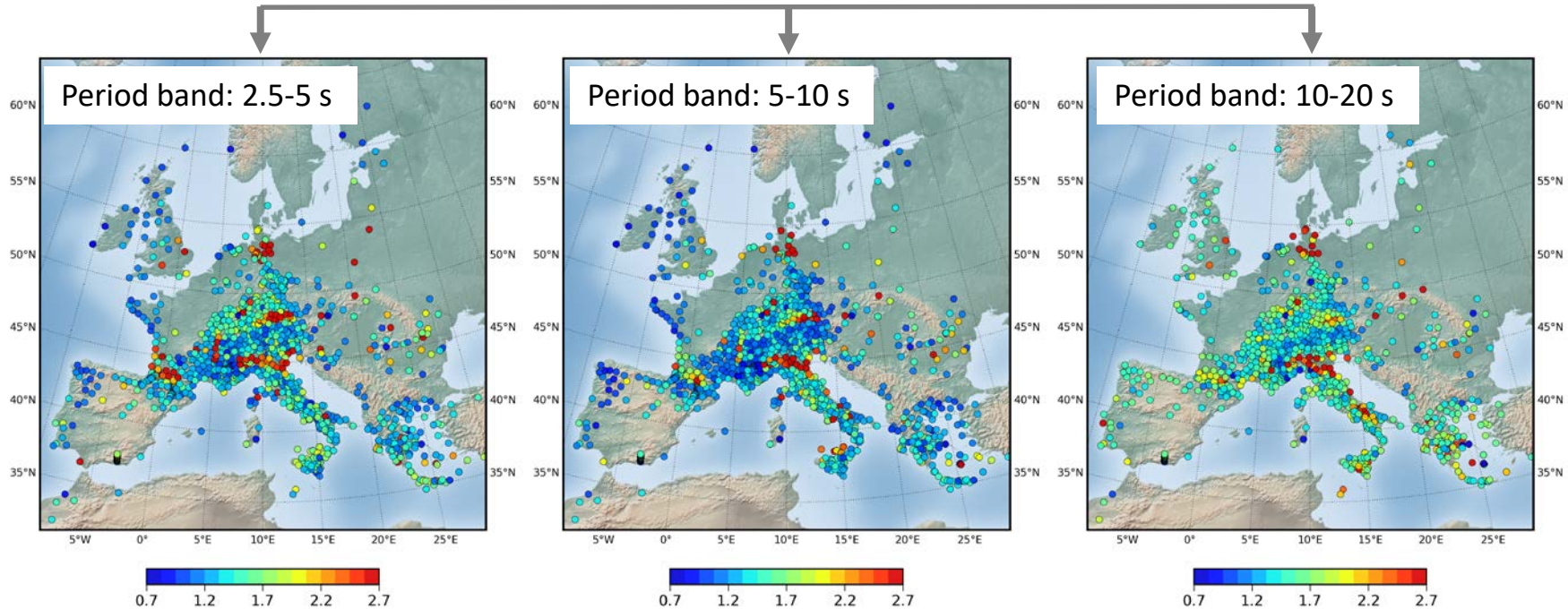
where λ_i ($\lambda_1 > \lambda_2 > \lambda_3$) refers to the eigenvalues of the covariance matrix of the three components.



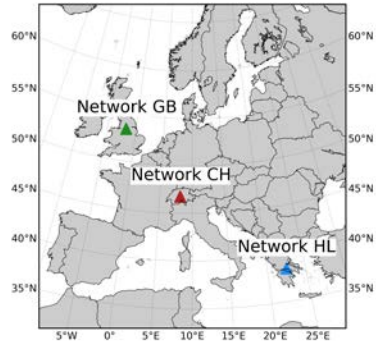
H/V decreases and rectilinearity increases in summer → higher influence of vertically propagating body waves?

Spatial distribution of total energy H/V ratio (mean over daily measurements 2011-2018)

Spatial variations are dominated by structure (but is the result of Rayleigh and Love waves)



Temporal variation of total energy H/V ratio (5 s - 10 s)



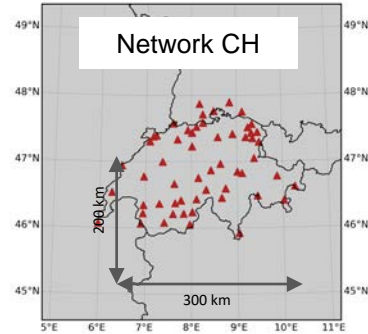
Daily energy $d(H/V)$

All years

Network GB

Network CH

Network HL

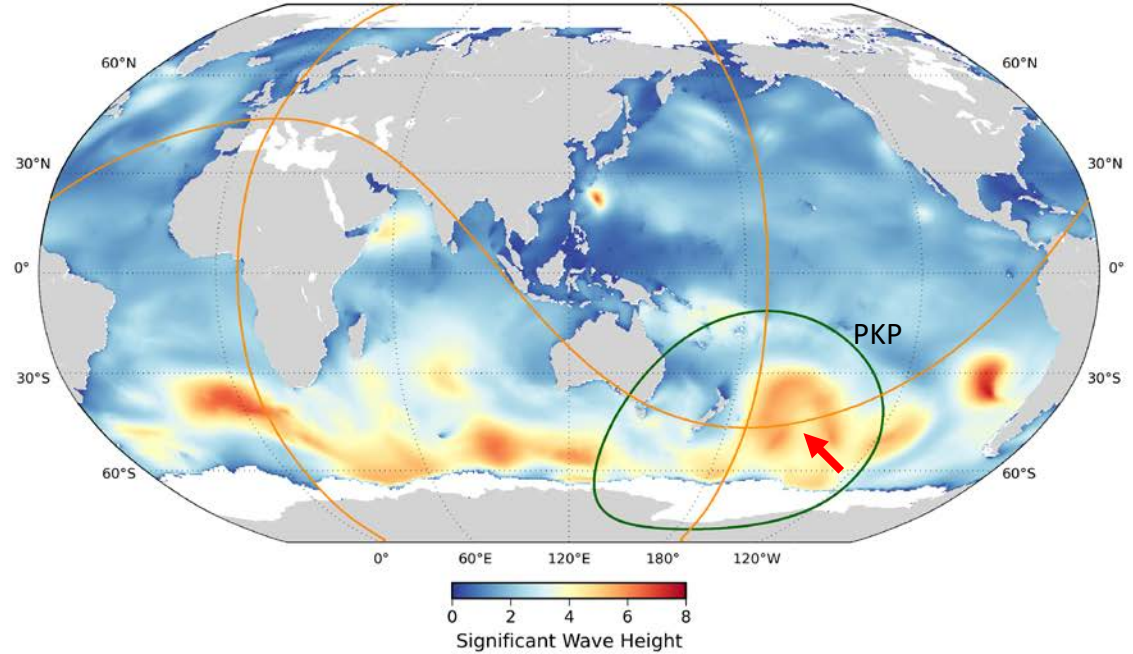
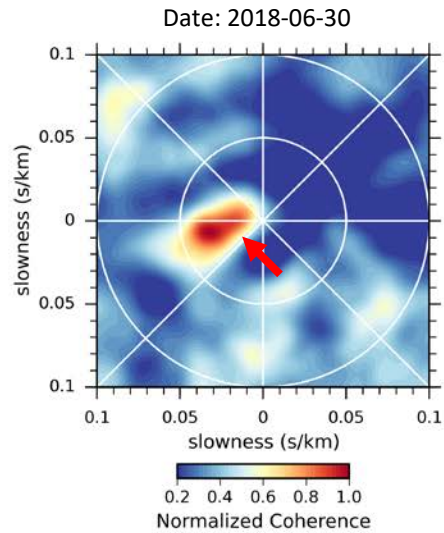


Daily energy $d(H/V)$

2018 for network CH

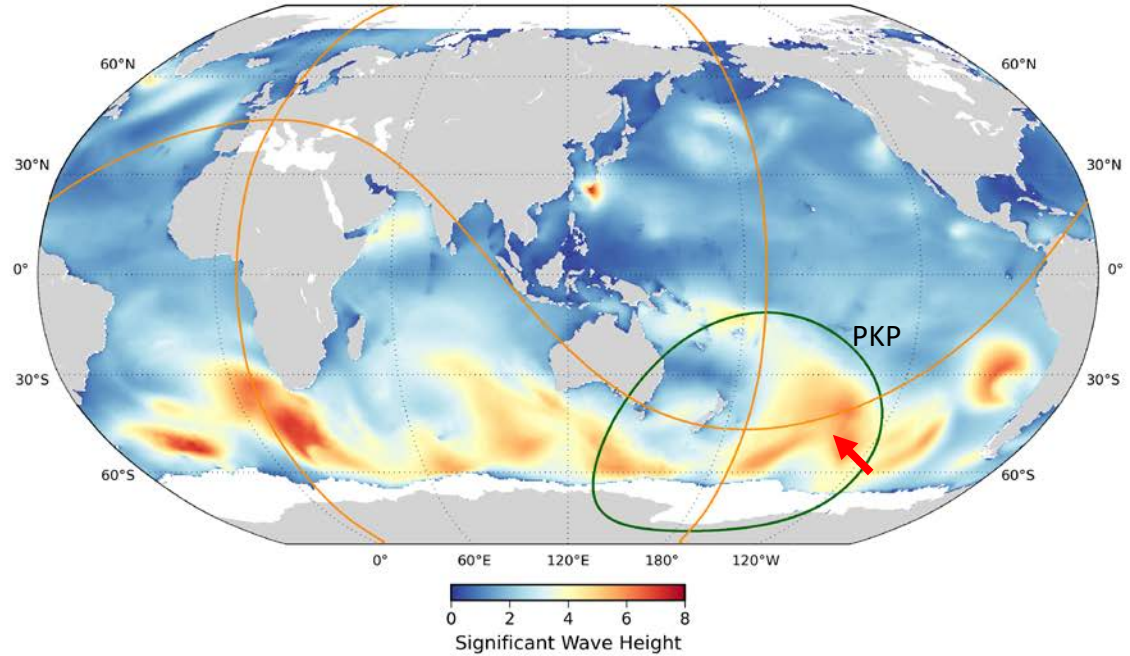
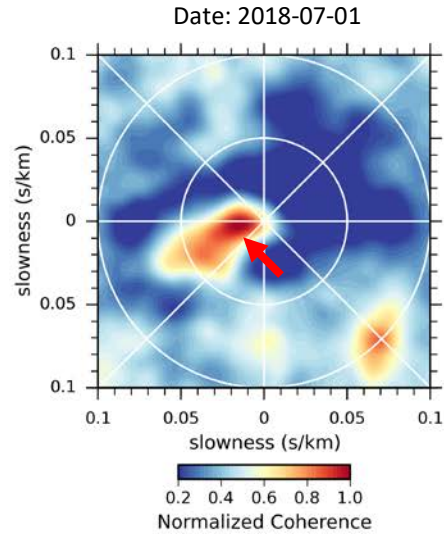
Significant decrease in H/V in summer for all networks – but large variations over time, and smaller effects for GB

Beamforming: body waves detected by network CH



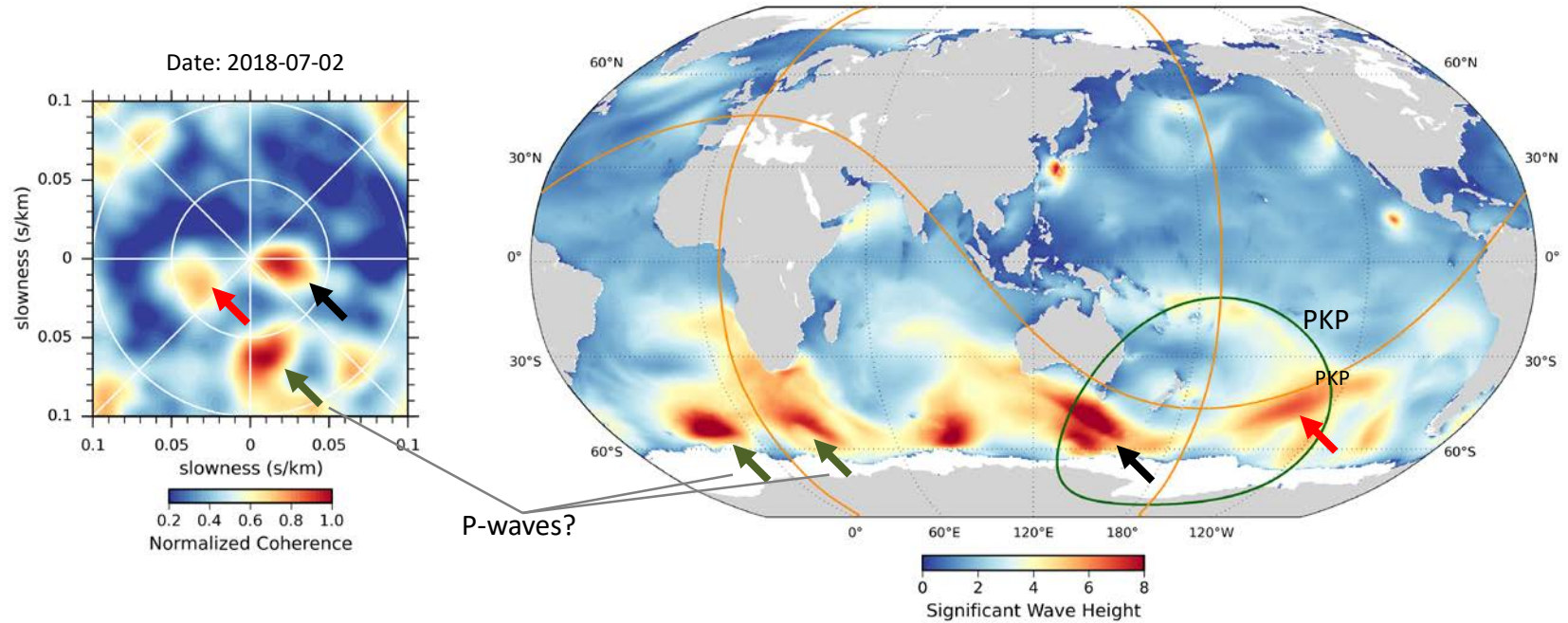
Clear observations of PKP wave from storm area in the south Pacific Ocean

Beamforming: body waves detected by network CH



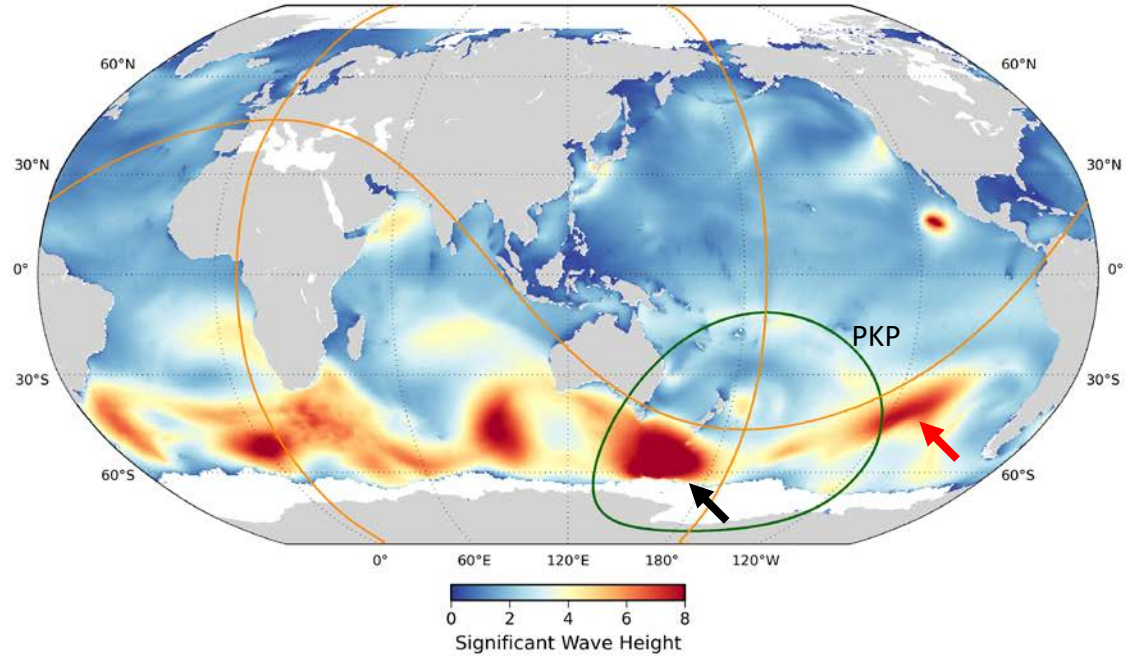
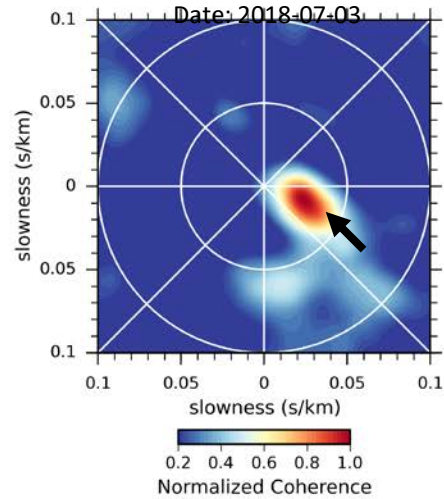
Clear observations of PKP wave from storm area in the south Pacific Ocean

Beamforming: body waves detected by network CH



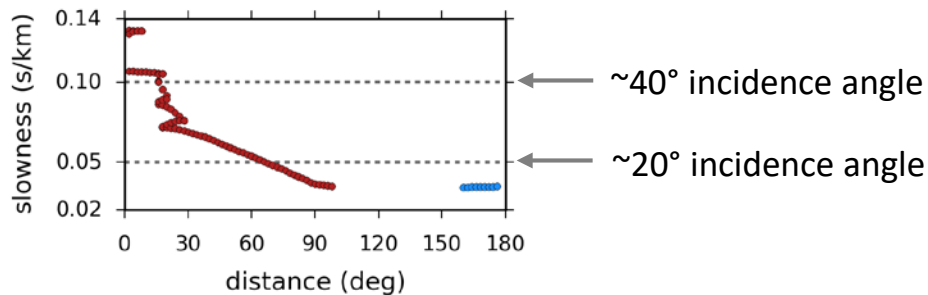
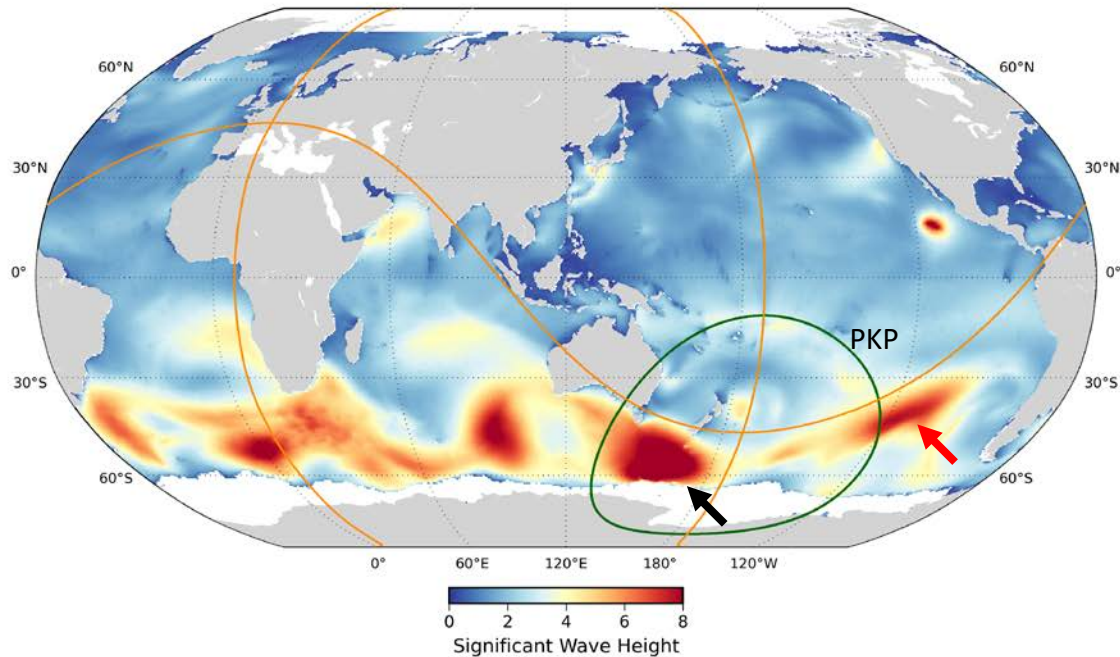
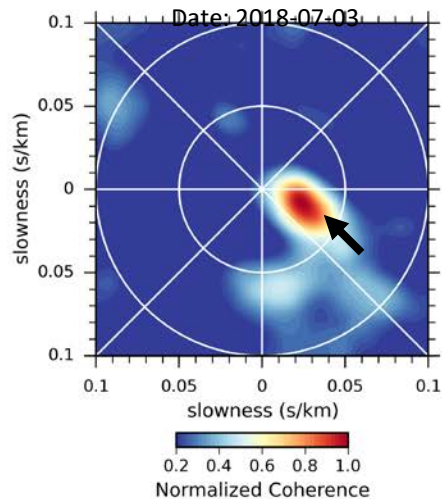
Clear observations of PKP waves from two storm areas in the south Pacific Ocean and from storm areas in South Atlantic

Beamforming: body waves detected by network CH



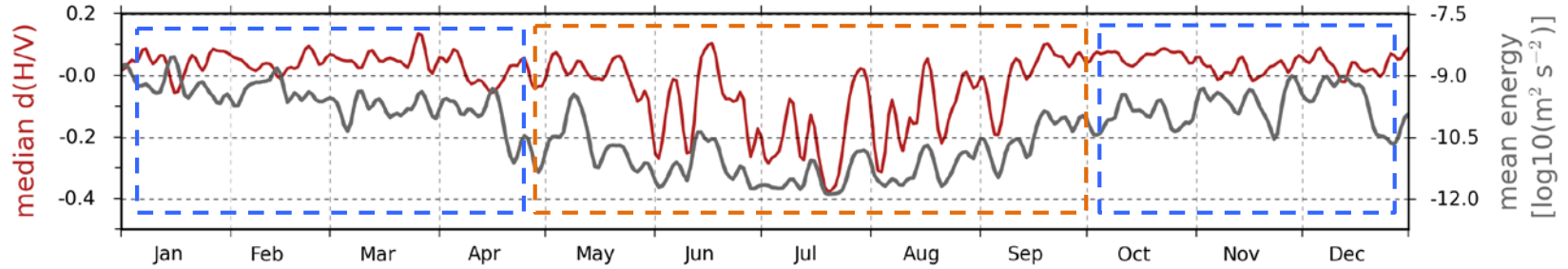
Clear observations of PKP wave from storm area in the south Pacific Ocean

Beamforming: body waves detected by network CH



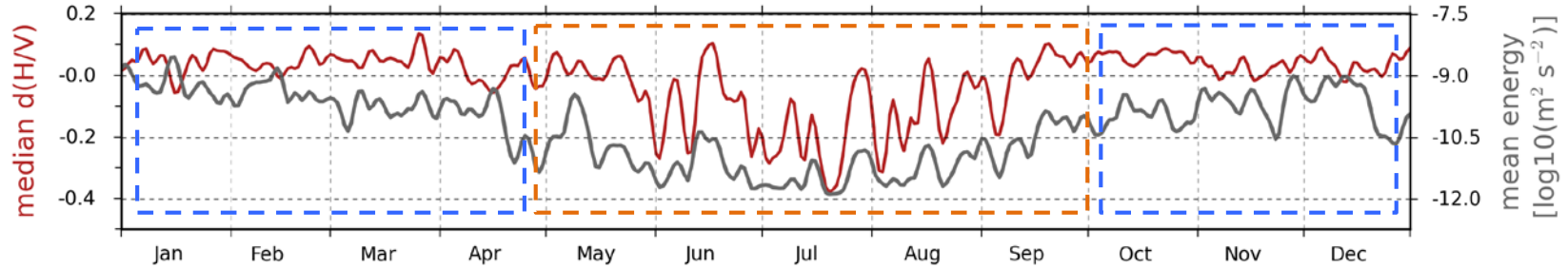
PKP can be estimated from slowness $p < 0.05$ s/km
P can be estimated from 0.05 s/km $< p < 0.1$ s/km:
Proxy for Atlantic activity

Comparison of H/V and total Energy



Approximate expression of H/V ratio : $ratio_{HV} = \frac{S_H + P_H}{S_V + P_V + PKP}$, where S_H and S_V are surface waves, H and V are hor. and vert. energy.

Comparison of H/V and total Energy



Approximate expression of H/V ratio : $ratio_{HV} = \frac{S_H + P_H}{S_V + P_V + PKP}$, where S_H and S_V are surface waves, H and V are hor. and vert. energy.

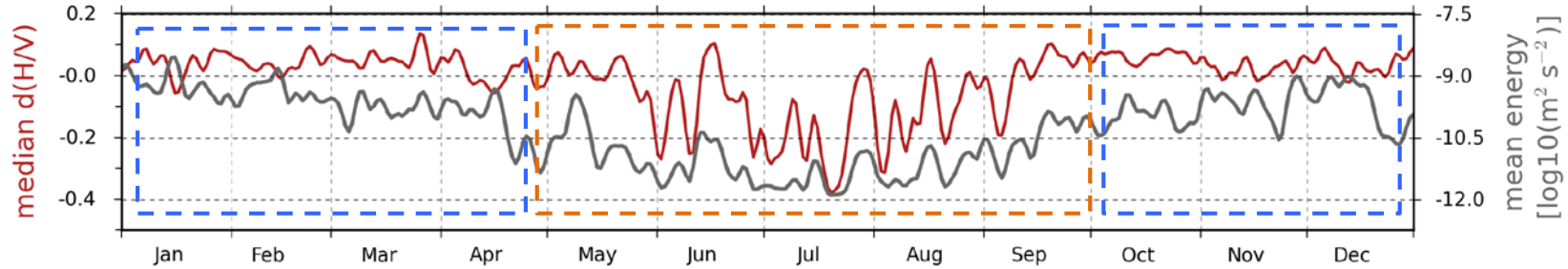
Small variations (and negative correlation?) in winter

Surface waves
dominate the
wavefield

$$ratio_{HV} \approx \frac{S_H}{S_V} \approx \frac{R_H + L}{R_V} = \frac{R_H + a * R_H}{b * R_H}$$

Love/Rayleigh ratio **a** dependent on total energy??

Comparison of H/V and total Energy



Approximate expression of H/V ratio : $ratio_{HV} = \frac{S_H + P_H}{S_V + P_V + PKP}$, where S_H and S_V are surface waves, H and V are hor. and vert. energy.

Small variations (and negative correlation?) in winter

Surface waves dominate the wavefield $\rightarrow ratio_{HV} \approx \frac{S_H}{S_V} \approx \frac{R_H + L}{R_V} = \frac{R_H + a * R_H}{b * R_H}$

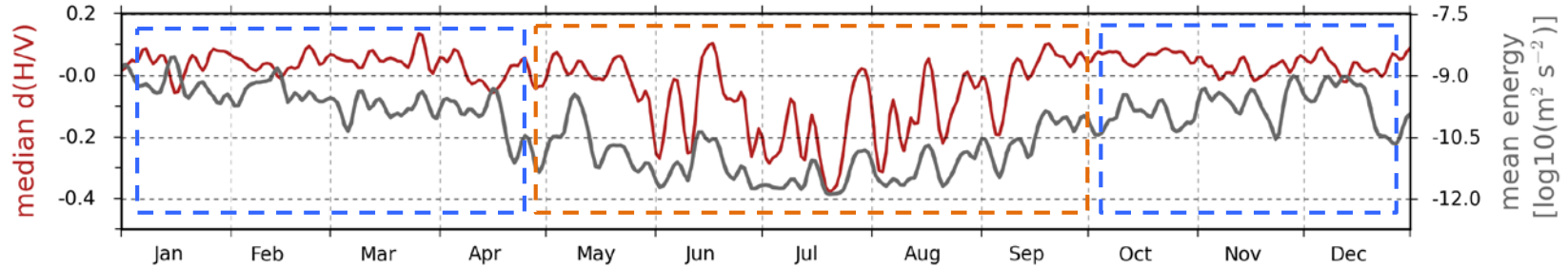
Love/Rayleigh ratio a dependent on total energy??

Strong variations and positive correlation in summer

Low Energy: Significant PKP waves $\rightarrow ratio_{HV} = \frac{S_H + P_H}{S_V + P_V + PKP}$

Increase of energy leads to increase of HV ratio, towards $\frac{S_H}{S_V}$

Comparison of H/V and total Energy



Approximate expression of H/V ratio : $ratio_{HV} = \frac{S_H + P_H}{S_V + P_V + PKP}$, where S_H and S_V are surface waves, H and V are hor. and vert. energy.

Small variations (and negative correlation?) in winter

Surface waves dominate the wavefield

$$ratio_{HV} \approx \frac{S_H}{S_V} \approx \frac{R_H + L}{R_V} = \frac{R_H + a * R_H}{b * R_H}$$

Love/Rayleigh ratio a dependent on total energy??

Strong variations and positive correlation in summer

Low Energy: Significant PKP waves $\rightarrow ratio_{HV} = \frac{S_H + P_H}{S_V + P_V + PKP}$

Increase of energy leads to increase of HV ratio, towards $\frac{S_H}{S_V}$

Interpretation of H/V ratio temporal variation (comparison with beampower ratio)

Working hypothesis: In summer H/V ratio is the combined result of surface waves in the Atlantic and PKP waves in the south Pacific:

- H/V increases if there are storms in the (north) Atlantic
- H/V decreases if there are storms in the south Pacific

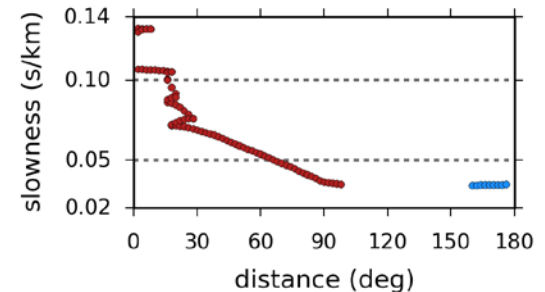
PKP P

Assumption: Energy (P)/Energy(PKP) is a proxy for the combined effect of North Atlantic and south Pacific

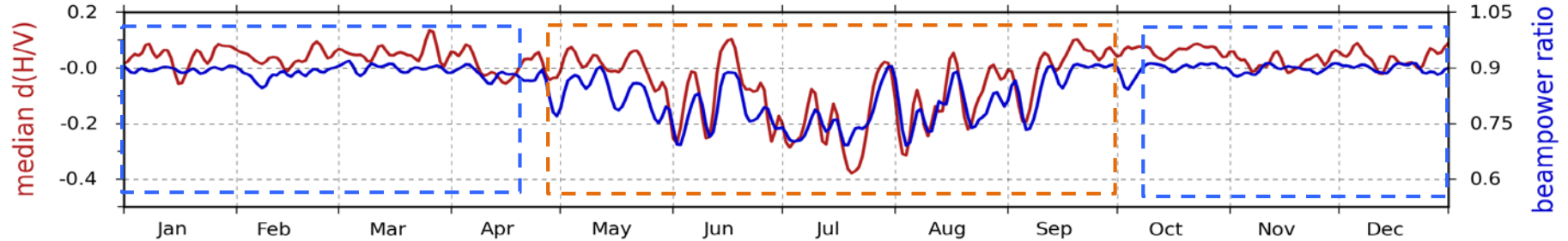
- P can be estimated from sum of beam power of slowness p : $0.05 \text{ s/km} < p < 0.1 \text{ s/km}$
- PKP can be estimated from beam power of slowness $p < 0.05 \text{ s/km}$

On all days we calculate

$$ratio_{beampower} = \frac{\text{Energy of beam } (0.05 < p < 0.1)}{\text{Energy of beam } (p < 0.05)}$$



Interpretation of H/V ratio temporal variation (comparison with beampower ratio)



Beampower ratio explains the temporal variation of H/V ratio in summer (! ?)

Investigations to be continued...

PkP P

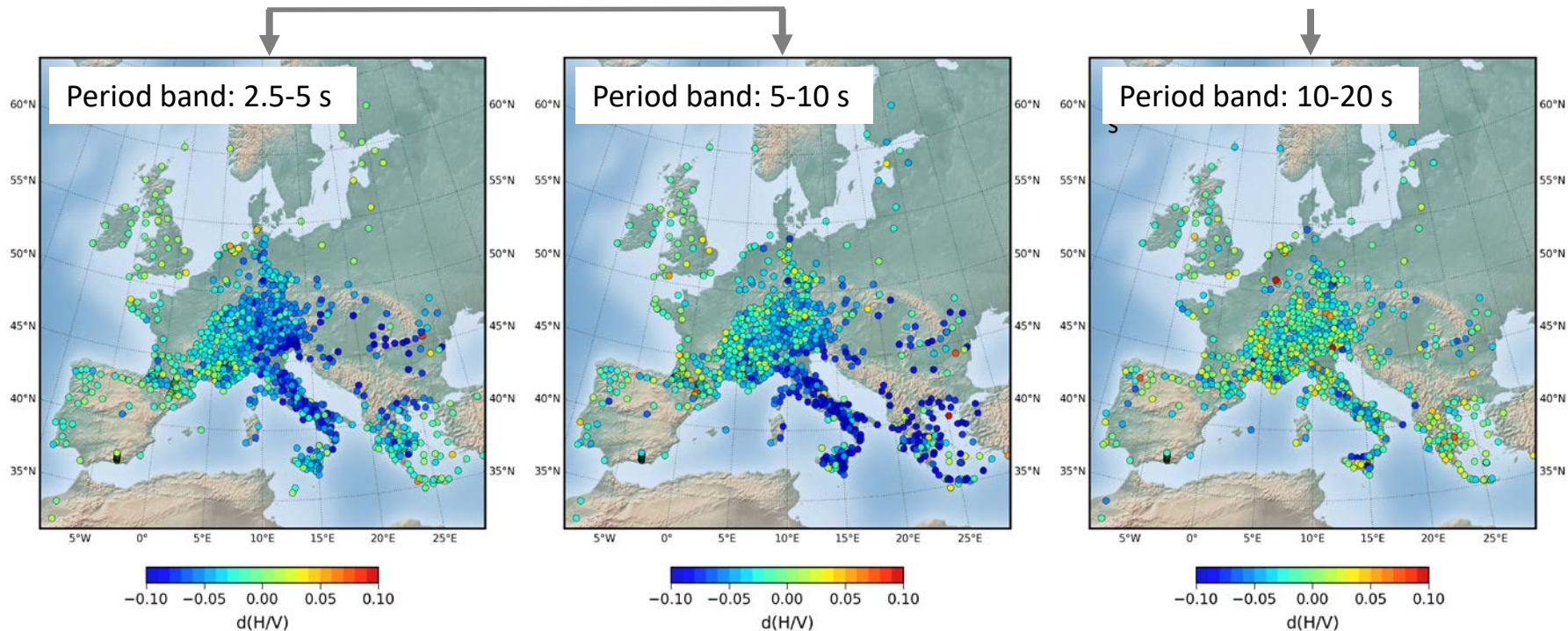
But $d(H/V) = \text{Summer } H/V - \text{average } H/V$ gives some insight into relative strength between PKP and surface waves

How does $d(H/V)$ vary spatially?

Mean $d(H/V)$ over daily measurements in summers (2011-2018)

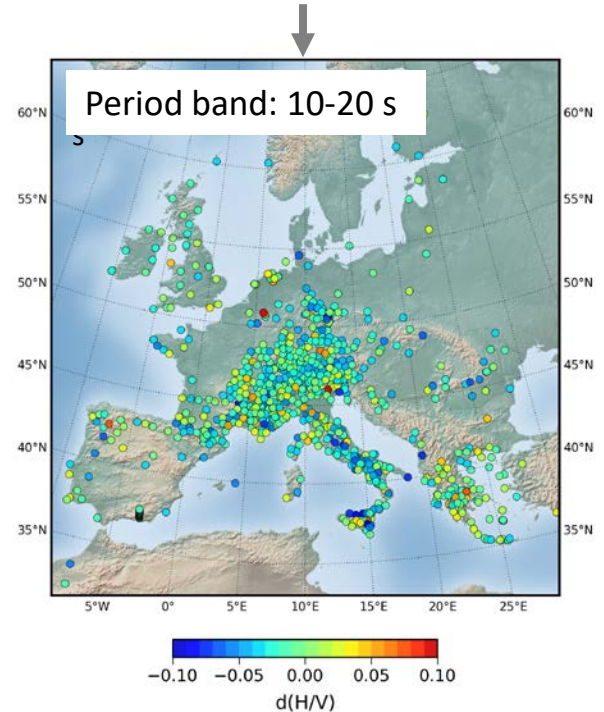
$d(H/V)$: effect dominated by the relative strength of local surface and teleseismic PKP waves.

$d(H/V)$ is insignificant; two options: no significant PKP waves or surface waves still dominant in summer



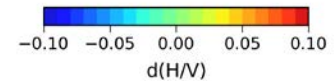
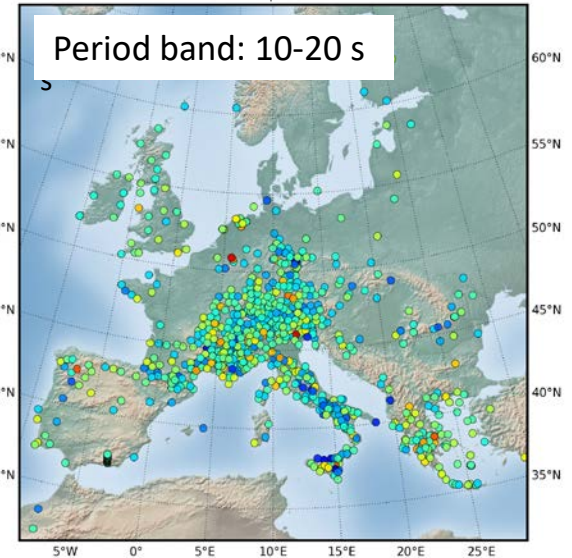
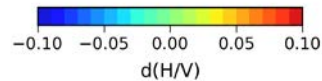
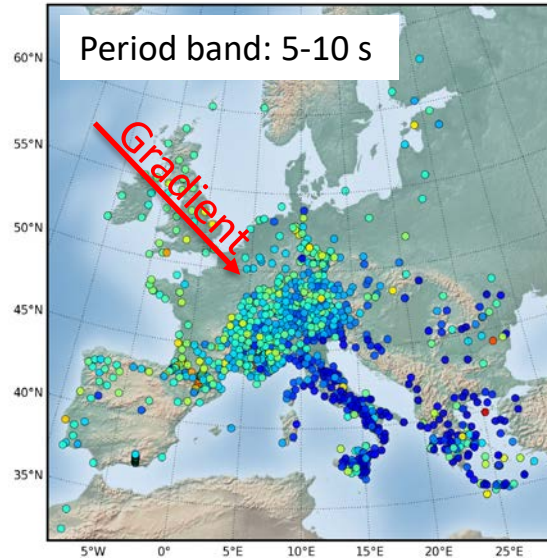
Mean $d(H/V)$ over daily measurements in summers (2011-2018)

$d(H/V)$ is insignificant; two options: no significant PKP waves or surface waves still dominant in summer



Mean $d(H/V)$ over daily measurements in summers (2011-2018)

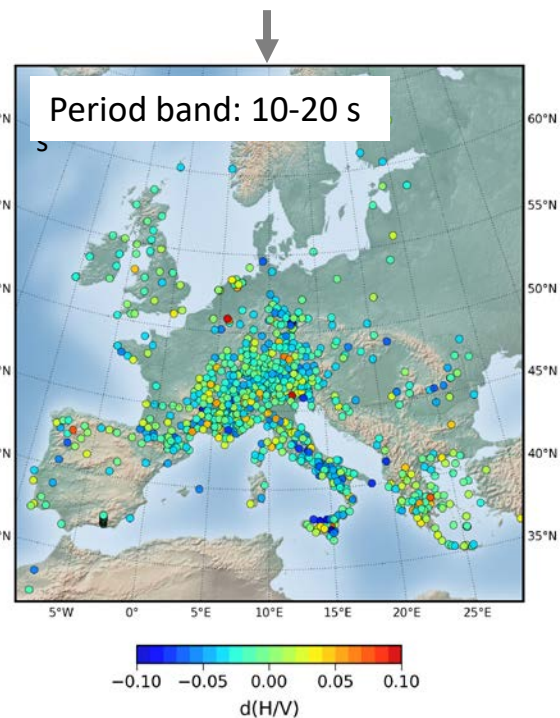
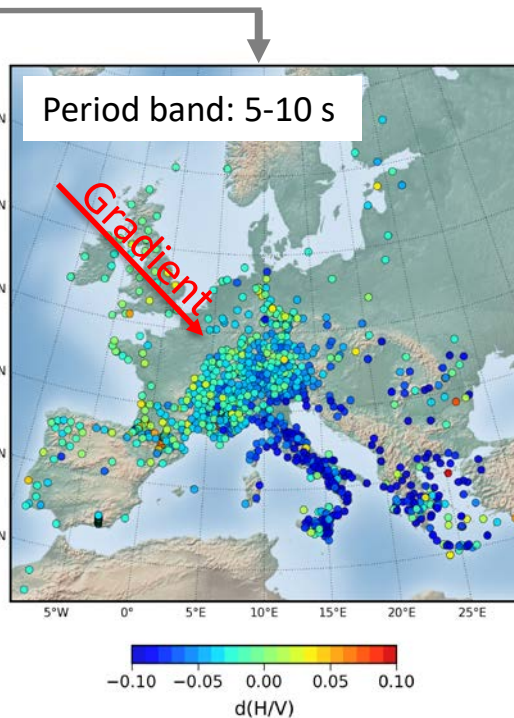
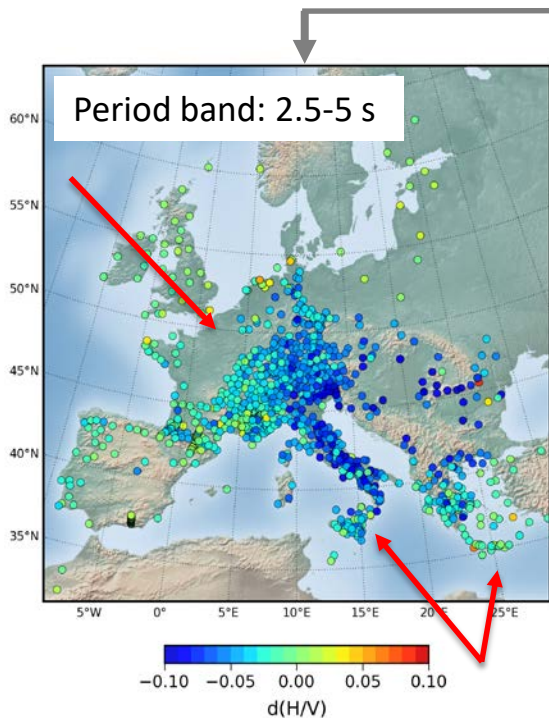
$d(H/V)$ is insignificant; two options: no significant PKP waves or surface waves still dominant in summer



Mean $d(H/V)$ over daily measurements in summers (2011-2018)

$d(H/V)$: effect dominated by the relative strength of local surface and teleseismic PKP waves.

$d(H/V)$ is insignificant; two options: no significant PKP waves or surface waves still dominant in summer



Conclusions

Mapping the noise field across Europe requires some use of single station measurements. In the framework of an underdetermined problem, we conclude that:

Using H/V in the first microseismic peak to invert for structure is a hazardous affair:

- Love waves are significant (and probably of higher amplitude on horizontal components than Rayleigh waves)
- Body waves are significant in summer even though surface waves dominate the wavefield coastal areas

3 component stations can give some insight as to the relative amplitudes of Rayleigh and Love waves

Variations of H/V can give some insight as to the relative strength of surface waves and body waves. We observe that:

- in the first microseismic peak, no such effects are visible: H/V does in general not have seasonal variations.
- in the second microseismic peak, PKP waves are sufficiently strong (as compared to the surface waves) in summer to modify H/V across most of Europe
- In the 5 s – 10 s period range, only the distance from the Atlantic Ocean is of relevance
- In the 2.5 s – 5 s period range, the distance to the Mediterranean coast is also of relevance